A PROPOSED ALGORITHM FOR RANGE AMBIGUITIES SUPPRESSION IN MULTI-STATIC SAR

Phuong Mai Nguyen Thi, Marc Rodriguez-Cassola, Gerhard Krieger

Microwave and Radar Institute, German Aerospace Center (DLR), Wessling, Germany

ABSTRACT

In a conventional synthetic aperture radar (SAR), good azimuth resolution and wide coverage pose contradicting requirements for the pulse repetition frequency (PRF). With a PRF tailored to a desired resolution, range ambiguities is then the main obstacle to a wide swath imaging. This paper proposes a method, based on a minimum variance distortion-less response (MVDR) beam former, to suppress range ambiguities, in range Doppler domain, via a coherent combination of echoes from multiple satellites maneuvering in a close formation. Numerical results in L band confirm validity of the approach. Limits of the technique and main difficulties in improving suppression performance are also discussed.

Index Terms**—** Range ambiguities, multi-static SAR, across-track formation, digital beam forming

1. INTRODUCTION

In SAR imaging, to achieve a good azimuth resolution basically requires a high PRF, which in turn allows the imaging of a non-unambiguous swath much smaller than demand [1]. Approaches to break this fundamental limit, to the author's best understanding, could be categorized in a group of processing orientation [2], [3], i.e. to eliminate ambiguities, and a group of system design, i.e. to control the amount of ambiguities via careful designed operation modes or parameters, like spotlight SAR. The main drawback in processing-oriented approaches is a lack of the demonstration of suppression technique for a distributed scene; while in system design group, combination of several modes for both resolution and coverage is not possible. Success of bi-static SAR acquistion [4] encourages a switch in attention to a multi-static system due to its advantages of cost effectiveness, system reliability, and possibility in incorporating multiple missions. A multi static SAR system try to achieve simultaneously resolution and coverage by combining information from multiple receivers, either in a same platform [5] or in distributed platforms [6], [7]. However, there is some degree of uncertainty to evaluate the system performance as conclusions, in many cases, are derived mainly via system parameters analysis.

We try to solve all above issues in our proposed approach. Briefly, we propose a multi static system with an image combination scheme. Both coverage and resolution are simultaneously satisfied by operation parameters, i.e., PRF and antenna pattern. Consequently, the remaining issue to address is range ambiguities elimination, which is possible, shown later in the following sections, via coherent combination of echoes from multiple receivers. We firstly recall properties of range ambiguities in the next section, then present a functional diagram demonstrating processing steps in range ambiguities suppression. Numerical results of suppression performance tested at multiple point-like targets over a swath of 120 km will be presented next. General conclusion concludes the paper.

2. RANGE AMBIGUITIES

Range ambiguities, by definition [8], refer to the occurrence of echoes from unintended scatterrers illuminated in an interval preceding and succeeding the illumination time of the main signal. It is due to side-lobes in the radiation pattern, as shown in the figure 1, or antenna footprint covering a region larger than the unambiguous one limited by PRF. Positions of such ambiguous scatterrers are defined via that of its associating target, R_0, and an ambiguity order m, [8]

$$R_m = R_0 + m \cdot \frac{c}{2 \cdot \mathrm{PRF}}, \tag{1}$$

Here, m means the difference in illumination time of an ambiguity and its target is $m \cdot \mathrm{PRF}$. Since ambiguous echoes arrive at a same time as that of the main signal, ambiguous point registers at a same range of the target, but exhibits a different Doppler rate [9]. This difference, which is difficult to observe around zero Doppler frequency, becomes obvious at the edge of the aperture, shown in fig. 2(a); leading to dispersed focused image, shown in fig. 2(b). (simulation parameters could be referred in the table 1). Usually, the azimuth focusing with mismatched Doppler rate reduces ambiguous energy significantly. However, residual ambiguous energy becomes noticeable when original range ambiguities-signal-ratio (RASR) is high. For an example, over 0 dB, which is usually found in a case of high PRF, i.e., good azimuth resolution.

The task of ambiguities suppression is challenging, mostly due to the slight difference in Doppler rates of the main signal and its ambiguous counterparts. Intuitively, one can prevent the occurrence of range ambiguities by forming nulls in the ambiguous angle of arrival. Alternatively, another way to exploit such spatial diversity is in phase of echoes entering an additional receiver located in a proximity of the main sensor. The reason for a close distribution become clear with analysis in the next section. Compared to the main sensor, useful and ambiguous echoes will travel extra distances of ΔR_0 and ΔR_m, respectively, to the additional sensor. Obviously, $\Delta R_0 \neq \Delta R_m$ would reflect in echoes phases, based on which a set of weighted coefficients can be designed to suppress range ambiguities.

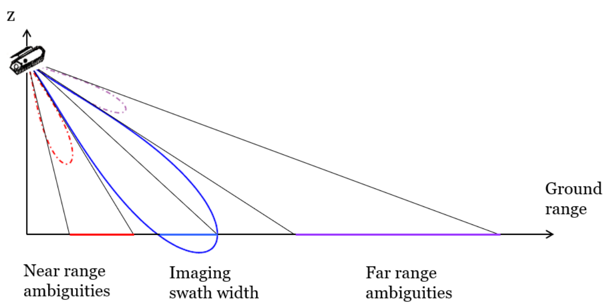

Fig. 1: Range ambiguities definition

Table 1: Simulation parameters

Parameter	**Value**
Carrier frequency [GHz]	1.25
Azimuth resolution [m]	2
Doppler bandwidth [Hz]	3800
Chirp bandwidth [MHz]	40
Orbit height [km]	550
Incidence angle of a point of interest [deg]	35.73
Slant range of interest [km]	664.15

(a) (b)

Fig. 2: Magnitude of (a) interest signal mixed with range ambiguities in range Doppler domain, and (b) focused ambiguous image. The horizontal and vertical axes correspond to range cell migration (in m) and Doppler frequency (in Hz)

3. PROPOSED RANGE AMBIGUITIES SUPPRESSION ALGORITHM

We consider here multiple satellites flying in a close formation: one satellite plays a role of both transmitter and receiver, called hereafter as TRx, the other are receive-only satellites. We assume that all satellites are separate in the elevation direction and altitude only, i.e., satellites share a same along-track coordinate. This configuration offers an advantage of phase center jump avoidance.

It's worth to consider a little bit range ambiguities characteristics in another receiver. Considering a range ambiguity as a mis-registered scatterer, in the TRx, it occupies a same range as the interest signal. In another receiver, depending on a distance to the TRx, such range ambiguity may or may not occupy a same range as the interest signal, while this interest signal, in turn, may or may not occupy the same range as that in the TRx. In the most general case, signal and ambiguities at a receive-only satellite have slightly different range references and Doppler rates compared to those at the TRx. Also, the difference becomes more noticeable with in far ranges than in near ranges.

We consider here the case that in a receive-only satellite, ambiguous and main signal still co-register, which is achieved only when receive-only satellites are located in a proximity around the TRx. Possible migration between signals in TRx and another receiver is compensated via slightly different range matched filter. Ambiguous signal are then suppressed in range Doppler domain employed the minimum variance distortionless response (MVDR) [10]. Specifically, a MVDR beam is designed at each Doppler frequency. The way to derive manifold vectors can be found in [11], where signal spectrum in our setup, is treated as azimuth-invariant bi-static and can be well approximated via the method of inverse series [12]. Formula of a MVDR beam can be found in [10]. The approach at this stage mainly focuses on demonstrating the suppression feasibility. The following diagram illustrates steps in data processing.

4. NUMERICAL RESULTS

Here, we demonstrate the capacity to suppress range ambiguities based on the above-mentioned scheme via simulation results in L band. There are, in total, four satellites employed with relative distances to the TRx, assuming unchanged during the reception time, shown in the **Table 2**. Suppression capacity is tested at three points of interest located at incidence angles of 35.7, 40.0, and 44.3 degrees. A flat spherical Earth model is used, and all satellites follow a linear movement with a same velocity vector. For distance measurement, we chose a Cartesian coordinate system with origin at the nadir when the TRx locates at the shortest distance to illuminated points, x axis is parallel to the TRx's velocity vector.

Figures 4 - 6 show suppression performance, given the op-

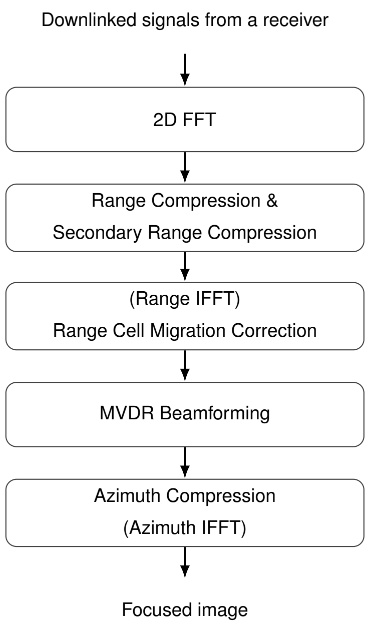

Fig. 3: A block diagram of processing steps

erating parameters listed in the tables 1 and 2. In each figure, sub-figures (a) and (c), respectively, show original magnitudes of range ambiguities and the desired signal; sub-figures (b) and (d), respectively, show magnitudes of suppressed range ambiguities and reconstructed signal. The x and y axes correspond to range cell migration (in m) and Doppler frequency (in Hz). It is observed, in all cases, that signal magnitudes remain nearly unchanged, while ambiguities magnitudes decrease reasonably, with measured MVDR-applied RASR at near, mid, and far-field positions are, respectively, -13.5 dB, -11.8 dB, 0.24 dB. These results confirm that the applied beam has worked.

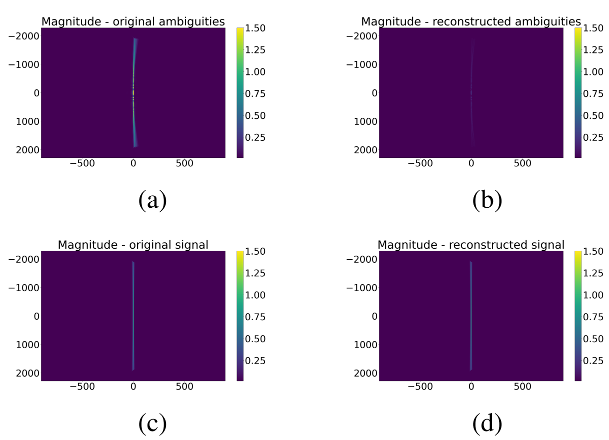

Fig. 4: Original and reconstructed ambiguities and signal at an incidence angle of 35.7 degrees

Table 2: System parameters to simulate suppression performance along a swath (ground range) of 120 km

Parameter	**Value**
Swath width [km]	120
Incidence at steering direction [deg]	40
Antenna height [m]	1.82
Antenna length [m]	3.33
Relative positions (w.r.t the TRx) of receive-only satellites ($[x, y, z]$) [m]	[0, -10, 5], [0, 10, 0]), [0, 5, 5],
White noise power [dB] (under signal peak power)	-3
Original RASR at examined points [dB] (in the order of near, mid, far ranges)	3.67, 0.5 , 9.8

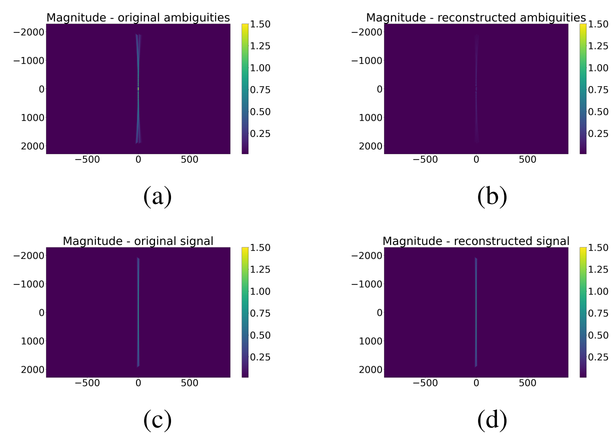

Fig. 5: Original and reconstructed ambiguities and signal at an incidence angle of 40.0 degrees

5. CONCLUSION

The analysis and simulation result have demonstrated that, an ambiguities-free image at a good resolution is achievable via a proper image reconstruction scheme employing signals from multiple satellites in cross-track formation. Deeper insight of reconstructed image is necessary to ensure that beam forming does not cause any distortion.

Also, its important to make sure residual energy in suppressed ambiguities falls below a threshold set by SAR image quality, i.e, -20 dB under signal power, which is not satisfied in the results above. It then leads to an important question of number of additional receivers and their distribution. Another aspect has not been mentioned in this paper is an efficient implementation of ambiguities suppression for a whole interest swath.

It's well-known that MVDR beam performance depends on the spatial correlation between the useful and interference

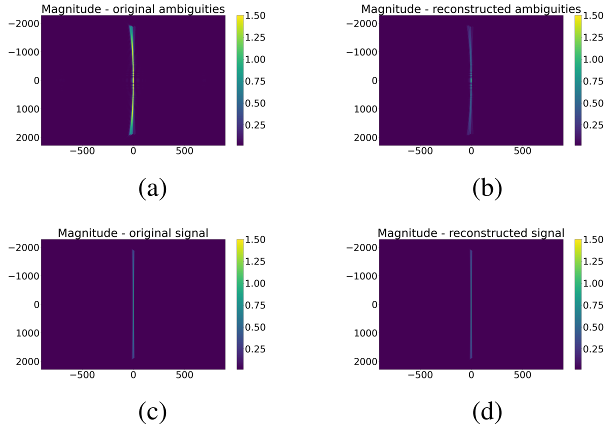

Fig. 6: Original and reconstructed ambiguities and signal at incidence angle of 44.3 degrees

signals [10]. This correlation is in turn mainly determined, in our case, by the across-track baseline. Simultaneously, an accuracy in satellites's position control, at this stage, is not perfect. Hence, it's of immense practical importance to analyze effect of fluctuation in satellites positions on the quality of suppression performance. All the issues are intended to be addressed in future papers.

6. REFERENCES

[1] A. Freeman, W. T. Johnson, B. e. a. Huneycutt, R. Jordan, S. Hensley, P. Siqueira, and J. Curlander, "The myth of the minimum sar antenna area constraint," *IEEE Transactions on Geoscience and Remote Sensing*, vol. 38, no. 1, pp. 320–324, 2000.

[2] A. Moreira, "Suppressing the azimuth ambiguities in synthetic aperture radar images," *IEEE Transactions on Geoscience and Remote Sensing*, vol. 31, no. 4, pp. 885–895, 1993.

[3] J. Dall and A. Kusk, "Azimuth phase coding for range ambiguity suppression in sar," in *IGARSS 2004. 2004 IEEE International Geoscience and Remote Sensing Symposium*, vol. 3, pp. 1734–1737, IEEE, 2004.

[4] M. Rodriguez-Cassola, *Bistatic synthetic aperture radar data processing*. PhD thesis, 2012.

[5] F. Q. de Almeida, M. Younis, P. Prats-Iraola, M. Rodriguez-Cassola, G. Krieger, and A. Moreira, "Slow pulse repetition interval variation for high-resolution wide-swath sar imaging," *IEEE Transactions on Geoscience and Remote Sensing*, vol. 59, no. 7, pp. 5665–5686, 2020.

[6] G. Krieger, N. Gebert, and A. Moreira, "Unambiguous sar signal reconstruction from nonuniform displaced phase center sampling," *IEEE Geoscience and Remote Sensing Letters*, vol. 1, pp. 260–264, 2004.

[7] N. Sakar, M. Rodriguez-Cassola, P. Prats-Iraola, and A. Moreira, "Azimuth reconstruction algorithm for multistatic sar formations with large along-track baselines," *IEEE Transactions on Geoscience and Remote Sensing*, vol. 58, no. 3, 2019.

[8] J. C. Curlander and R. N. McDonough, *Synthetic aperture radar*, vol. 11. Wiley, New York, 1991.

[9] F. Li and W. Johnson, "Ambiguities in spacebornene synthetic aperture radar systems," *IEEE Transactions on Aerospace and Electronic Systems*, vol. 19, no. 3, 1983.

[10] H. L. Van Trees, *Optimum array processing: Part IV of detection, estimation, and modulation theory*. John Wiley & Sons, 2004.

[11] P. M. Nguyen T, M. Rodriguez-Cassola, and G. Krieger, "Cross-platform range ambiguity rejection algorithm for multi-static sar constellations in elevation," accepted in EUSAR, 2022.

[12] Y. L. Neo, F. Wong, and I. G. Cumming, "A two-dimensional spectrum for bistatic sar processing using series reversion," *IEEE Geoscience and Remote Sensing Letters*, vol. 4, no. 1, 2007.